AIAA-98-0057

Relating Turbulence to Wind Turbine Blade Loads: Parametric Study with Multiple Regression Analysis

Tina Kashef and Steven R. Winterstein
Civil Engineering Dept., Stanford University

Abstract

Different wind parameters are studied to find a set that is most useful in estimating fatigue loads on wind turbine blades. The histograms of rainflow counted stress ranges are summarized through their first three statistical moments and regression analysis is used to estimate these moments in various wind conditions. A systematic method of comparing the ability of different wind parameters to estimate the moments is described and results are shown for flapwise loads on three horizontal axis wind turbines(HAWTs). In the case of two of these turbines, the stress ranges are shown to be highly correlated with a turbulence measure obtained by removing a portion of the low-frequency content of the wind.

Introduction

This paper considers how well various wind parameters—such as the mean wind speed and various turbulence measures—can be used to estimate fatigue loads on wind turbine blades. We first describe a general approach for this purpose, which can (1) conveniently summarize fatigue load data, and (2) systematically test their statistical correlations with various wind parameters. The term "fatigue loads" in this paper refers to the amplitudes of the rainflow counted stresses. Separating the wind and load data into 10-minute wind "events," our approach proceeds in two stages:

- Observed frequencies (histograms) of rainflow-counted load amplitudes are summarized through their first three statistical moments: mean, standard deviation, and skewness. Note that these are the statistics of the load amplitudes rather than the stress time history, e.g., the mean stress refers to the mean amplitude of the rainflow counted stresses, and not the average stress.
- Concepts from multiple statistical regression are applied to systematically study how well various wind parameters are able to estimate the various blade load moments.

Our previous work has suggested that, within a particular wind event, this 3-moment load description often carries sufficient information to accurately predict the underlying load histogram over the range of interest (e.g., Winterstein and Lange, 1995). Previous studies have used simpler 1- and 2-parameter models, at least in the high-amplitude region. Examples include the exponential model (e.g., Jackson, 1992; Kelley, 1995), the Rayleigh model (e.g., Veers, 1982), and more general Weibull models. Our 3-moment models use a "quadratic Weibull" distribution (Lange and Winterstein, 1996), which includes these various 1- and 2-parameter models as special cases.

We therefore study here the variation of these 3 load moments *across* multiple wind events, to conveniently describe general trends in mean loading, load distribution shape, etc. Results are shown for flapwise loads on three different horizontal axis wind turbines (HAWTs). We show how techniques from multiple regression analysis can be used to evaluate and rank the abilities of various wind parameters—e.g., mean wind speed V and turbulence intensity I— to "explain" the observed variability in load moments. Previously, some load statistics for a single HAWT showed weak dependence on I (Veers and Winterstein, 1997); a resulting question is whether a "more informative" turbulence intensity I can be achieved by removing some portion of the low-frequency wind content (e.g., Connell et al, 1988). Regression concepts are applied here to systematically study the best choice of filtering, and hence the most informative definition of I.

Note that our focus here lies on demonstrating general methods to estimate load statistics from wind parameters, and applying them to cases where

wind measurements are available from only a single anemometer. Thus we seek not the best possible turbulence parameters, but rather the best descriptors available from the limited wind data commonly at hand. We recognize that improved turbulence characterization would follow from knowledge of multiple wind speed components across various elevations (e.g., Kelley, 1993). This may prove a useful avenue of further study, in cases where sufficient inflow data are available.

Background

Fatigue lifetime calculations for members subject to cyclic loads are usually performed using S–N curves and Miner's rule. For members subject to constant amplitude loading, the number of cycles to failure is related to the stress amplitude S by:

$$N(S) = \frac{1}{cS^b} \tag{1}$$

in which c and b are material properties. In the case of load histories that are composed of cycles with varying amplitudes, for each cycle of amplitude S_i Miner's rule assigns fatigue damage

$$D_i = \frac{1}{N(S_i)} = cS_i^b \tag{2}$$

The total damage D_{tot} in time T is then found by summing the damage increments D_i over all $N(T)$ stress cycles:

$$D_{tot} = \sum_{i=1}^{N(T)} D_i = \sum_{i=1}^{N(T)} cS_i^b \tag{3}$$

For statistical purposes, it is convenient to rewrite this result as

$$D_{tot} = \dot{D} \cdot T \tag{4}$$

in which $\dot{D}$ denotes the average damage rate per unit time. From Eqs. 3-4, $\dot{D}$ can be expressed as

$$\dot{D} = cf_0\overline{S^b} \tag{5}$$

in which f_0=$N(T)/T$ is the mean rate of stress cycles per unit time, and $\overline{S^b}$=$\sum_{i=1}^{N(T)} S_i^b/N(T)$ is the b-th statistical moment of the stress history. An advantage of this form is that the terms f_0 and $\overline{S^b}$ should stabilize as time grows, and hence are convenient quantities to estimate from limited stress data.

Short-Term versus Long-Term Damage Rates. For purposes of statistical estimation, it may also be useful to note that quantities such as f_0 and $\overline{S^b}$ will vary with gross wind conditions; e.g., as a function of the mean wind speed V. Denoting these quantities as $f_0(V)$ and $\overline{S^b(V)}$, one can define an analogous *short-term* damage rate $\dot{D}(V)$ over a steady-state wind event (with mean wind speed V):

$$\dot{D}(V) = cf_0(V)\overline{S^b(V)} \tag{6}$$

The long-term damage rate, $\dot{D}$ in Eq. 5, can then be found as

$$\dot{D} = \int \dot{D}(V)p(V)dV \tag{7}$$

which weights the short-term damage rate $\dot{D}(V)$ by the long-term probability, $p(V)dV$, of encountering wind speeds between V and $V+dV$. (If the damage rate $\dot{D}$ is instead modelled as a function of both V and turbulence intensity I, the above result becomes a double integral weighted by the joint probability $p(V,I)$ of various V–I combinations.)

This approach has the advantage of splitting the problem into two distinct parts:

1. The "short-term problem" of finding $\dot{D}(V)$=$cf_0(V)\overline{S^b(V)}$, which is a characteristic of the machine and independent of the site; and

2. The "long-term problem" of finding $p(V)$, which is a characteristic of the site and independent of the machine.

Although $\overline{S^b(V)}$ in equation (6) can be calculated directly from the observed stress ranges in the wind event, the result may vary greatly for different realizations of the same wind condition. This is especially true in the case of large values of the exponent b, due to the sensitivity of higher moments to rare, high stress cycles. By calculating the b-th moment instead from a smooth, continuous probabilistic model fitted to all stresses, one can hope to avoid this problem. In effect, fitting a distribution seeks to compensate for the lack of data in a particular wind event by using the body of the data and an assumption about the shape of the distribution to estimate the tail.

Basic Regression Model and Sample Results

We first review here some basic concepts from linear regression. The simplest model seeks to estimate an "output" variable Y from a linear function $\hat{Y}(X)$ of a single "input" variable X:

$$Y = \hat{Y}(X) + \epsilon\,; \quad \hat{Y}(X) = \alpha + \beta X \tag{8}$$

(In our case, Y is some statistic of the blade loads while X describes some property of the wind climate.) In general the error, $\epsilon = Y - \hat{Y}(X)$, is assumed to have zero mean and constant variance σ_ϵ^2 for all X. (Equivalently, given knowledge that $X=x$ the outcome of Y is said to have "conditional mean" $\hat{Y}(x)=\alpha+\beta x$ and "conditional variance" σ_ϵ.) The extension to p "input" variables is direct: βX in Eq. 8 is replaced by $\beta_1 X_1 + ... + \beta_p X_p$.

Linear regression methods then provide various results, including:

- $a, b_1, ..., b_p$=single ("point") estimates of the true but unknown parameters $\alpha, \beta_1, ..., \beta_p$.
- $\sigma_a, \sigma_{b_1}, ..., \sigma_{b_p}$=standard deviations associated with these estimates, as well as correlations between them.
- An estimate of σ_ϵ^2, and hence of the fraction of output variance, σ_Y^2, explained by the regression estimation $\hat{Y}(X)$:

$$R^2 = 1 - \frac{\sigma_\epsilon^2}{\sigma_Y^2} = 1 - \frac{\frac{1}{n_1}\sum_i [Y_i - \hat{Y}(X_i)]^2}{\frac{1}{n_2}\sum_i [Y_i - \overline{Y}]^2} \quad (9)$$

The first two items can be used to reflect the effects of limited data; e.g., to model a true parameter such as α as uncertain, with best estimate a and standard deviation σ_a. The CYCLES (FAROW) code (Jha and Winterstein, 1997) can propagate these effects through a fatigue reliability analysis, and hence can assess the reliability implied by various design load factors. The R^2 value, in turn, is used here to quantify the ability of various wind climate parameters—and their combinations—to "explain" the load statistic Y.

Note that the most common R^2 definition normalizes both sums in Eq. 9 by n_1=n_2=n, the total number of data. This ensures a minimal R^2 value of zero, arising when the best predictive line $\hat{Y}(X)$ is flat; i.e., always equal to the mean value $\overline{Y}$. A corresponding drawback is that this R^2 value will generally increase whenever an extra input variable X_i is included, nearing unity as collocation to all data is approached. To better reflect the true benefit of the variables from the data at hand, the so-called "adjusted" R^2 value is found from Eq. 9 by choosing n_1=$n-p-1$ and n_2=$n-1$, thereby achieving unbiased estimates of both numerator and denominator:

$$R^2 = 1 - \frac{\frac{1}{n-p-1}\sum_i [Y_i - \hat{Y}(X_i)]^2}{\frac{1}{n-1}\sum_i [Y_i - \overline{Y}]^2} \quad (10)$$

It is this "adjusted" R^2 we report here; this can (and does) sometimes decrease when an additional variable is added, suggesting no significant benefit based on the data at hand.

Single Wind Parameter. We first study the regression of a moment μ on mean wind speed V. The choice of the wind parameter follows standard practice. The functional shape used for the regression is a power-law expressed as:

$$\mu = \alpha(\frac{V}{V_{ref}})^\beta \quad (11)$$

This functional form, while permitting curvature in the regression line, ensures that no changes in trend occur outside the range of observations. The reference value V_{ref} normalizes the parameter V and renders it dimensionless. The relationship can be transformed to a linear form by taking logs of both sides:

$$\log\mu = \log\alpha + \beta(\log V - \log V_{ref}) \quad (12)$$

We choose $\log V_{ref}$ as the arithmetic mean of $\log V$, or equivalently, set V_{ref} equal to $\sqrt[n]{V_1 V_2 \dots V_n}$, the geometric mean of the data V's. This results in uncorrelated estimates of the regression coefficients $\log\alpha$ and β.

As an initial example, we will study the regression of the first moment using data obtained for the NPS machine. This is a two-bladed horizontal axis wind turbine (HAWT) with a rotor diameter of 17.8 meters and a power rating of 100 kilowatts. The data set consists of 20 10-minute segments of bending moment stress data and wind speed sampled at a frequency of 36 Hz. Although in this paper we focus only on the analysis of flapwise bending moments, our studies (Kashef and Winterstein, 1997) indicate that in the case of edgewise stresses the sum of the stress ranges, i.e., $f_0\overline{S}$, has a behavior that is more easily understandable than that of the mean $\overline{S}$ alone. Thus, for consistency we will study—in this paper as well—the sum $f_0\overline{S}$ instead of the mean.

Figure 1 shows the regression of $f_0\overline{S}$ performed using NPS flapwise stress data. The slope of the regression line shows a definite trend with V. However, there is still a large scatter about this line. The R^2 suggests the same: at .53, it shows that much of the variation in $f_0\overline{S}$ has not been accounted for by the trend in V. This leads us to seek a better explanation of these variations through the introduction of an additional wind parameter.

Multiple Wind Parameters. It seems reasonable to use, as an additional wind parameter, a measure of the wind turbulence. Traditionally, the turbulence intensity I—the coefficient of variation of

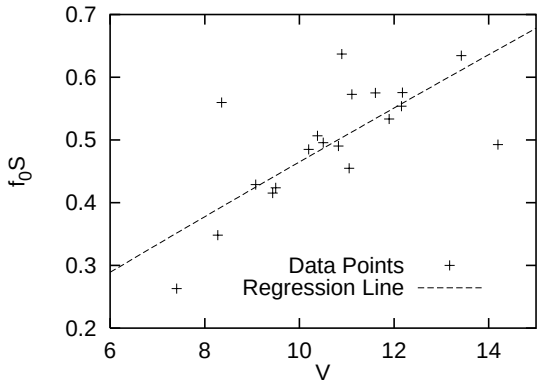

Figure 1: Regression of $f_0\overline{S}$ on mean wind speed.

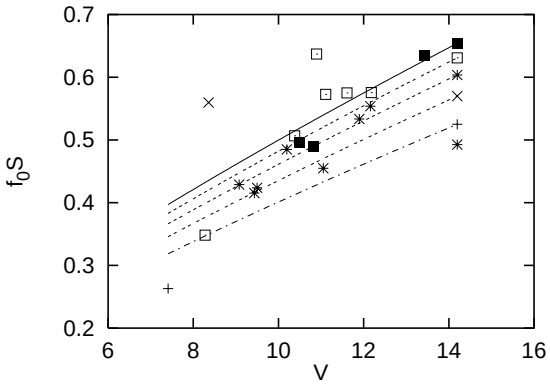

Figure 2: Joint regression of $f_0\overline{S}$ on V and σ_W plotted vs. V. The symbol at the far right of each line matches that used for plotting the data points corresponding to the same bin. Note that the top lines correspond to higher σ_W values.

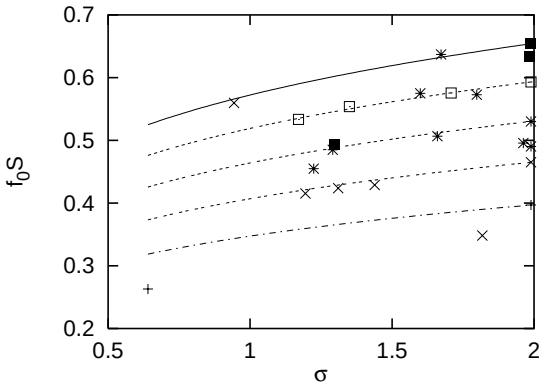

Figure 3: Joint regression of $f_0\overline{S}$ on V and σ_W plotted vs. σ_{high}. Note that the top lines correspond to higher V values

the wind speed—has been used for this purpose. From the mechanics of the problem, however, one would imagine that the amplitude of the wind fluctuations, as measured by the standard deviation of the wind speed σ_W, is more directly related to the stress amplitudes. For this reason we will use σ_W, rather than I, as a turbulence measure. The functional form used is a direct generalization of the one-parameter case:

$$\mu = \alpha(\frac{V}{V_{ref}})^{\beta_1}(\frac{\sigma_W}{\sigma_{W,ref}})^{\beta_2} \qquad (13)$$

Notice that, since a power law is used for the regression, the choice between σ_W and I will only have the effect of changing β_1 (by β_2 units). The difference between the two becomes evident later when we study single-variable power-laws in σ_W and I individually. Once again the function is transformed to a linear form by taking logs:

$$\log\mu = \log\alpha + \beta_1(\log V - \log V_{ref}) + \beta_2(\log\sigma_W - \log\sigma_{W,ref}) \qquad (14)$$

Choosing V_{ref} and $\sigma_{W,ref}$ as the geometric means of the data V's and σ_W's results in an estimate of the intercept α which is independent of the β's.

Figures 2 and 3 show the two-parameter regression of $f_0\overline{S}$ for the same data set. In order to plot the results, the V–σ_W plane has been divided into a 5×5 grid. Figure 2 shows the regression surface plotted vs. V at the midpoints of the bins in the σ_W direction. The data points have been similarly divided by bin in that direction. Notice that the regression surface seems to slope considerably with V, suggesting an important trend with this parameter. Figure 3 shows the same regression surface, now plotted vs. σ_W at the midpoints of the bins in the V direction. Notice the flatness of the curves in this plot, indicating that $f_0\overline{S}$ does not change considerably with the turbulence.

The relative importance of V and σ_W in the joint regression can also be studied by comparing the R^2 values calculated for each of these parameters individually. Single parameter regressions, such as that explained in the preceding section using V, can be performed with either σ_W or I as the wind parameter. The R^2 values thus obtained are reflected in Table 1. Comparison of these results indicates that R^2_V—the percentage of variation explained by using V alone—is not only much larger than both $R^2_{\sigma_W}$

and R_I^2, but is also effectively equal to the R^2 corresponding to the joint regression using both V and σ_W (or I). This result, also suggested by the regression surface plots, indicates little benefit from including either of the turbulence measures as an additional parameter.

Other Turbulence Measures

The considerable scatter remaining around the regression surface—reflected in the low R^2—could be an indication that single point measurements of the wind speed do not contain sufficient information to estimate the stresses in the blades and that, for example, additional information about the spatial variations of the wind speed is required (Kelley, 1993; Barnard and Wendell, 1997). It is also possible, however, that other parameters could be abstracted from the available wind speed measurements that would be better correlated with the stress data. We now introduce a systematic method of searching for such parameters.

The wind speed is composed of a wide range of frequencies, each of which contribute a part to the total variance. It is plausible, however, that the dynamics of the machine are mainly driven by the higher frequency components, and that the general shape of the stress range distributions, as reflected in their first few moments, would not be greatly influenced by the low frequency components. This observation suggests that removing long-term trends from the wind speed history before calculating its standard deviation may provide us with a better parameter for estimating the stress moments.

The idea of de-trending is not new. Linear detrending has been suggested for removing the long-term variations of the wind speed before (Connell et al., 1988). When used for the NPS data, this method increases the R^2 from .52 (for a joint regression on V and σ) to .55. This increase could be an indication that de-trending, in concept, is effective—one is tempted to believe that removing more than a linear trend may result in better parameters still.

Wind Parameter(s)	R^2
V	.53
σ_W	.31
I	.02
(V,σ_W) or (V,I)	.52

Table 1: Comparison of R^2 values for different wind parameters

Wind Parameter(s)	$f_{cut} = .005$ (Hz)	$f_{cut} = .15$ (Hz)
V	.53	.53
σ_{high}	.78	.90
I_{high}	.40	.56
(V,σ_W) or (V,I)	.76	.89

Table 2: R^2 values for different cutoff frequencies

The simplest and most direct way of reducing the contribution of long-term variations would be to completely remove a certain number of low-frequency components from the wind speed process before calculating the variance. This is equivalent to high-pass filtering the wind speed with a rectangular filter. Since the variance of a process is equal to the area under its power spectral density, the filtered variance σ_{high}^2 can be calculated by subtracting the area corresponding to the filtered frequencies (i.e., below the frequency cutoff) from the total variance. In this way, the standard deviation can be easily computed for successively increasing frequency cutoffs.

The question is now whether, by filtering out lower frequency components, we arrive at better turbulence parameters, and if so which cutoff provides the turbulence measure with the greatest power in estimating the stress distribution. To answer these questions, we have—for different cutoff frequencies—calculated the filtered standard deviation σ_{high} and its corresponding R^2 values. Table 2 shows the results for a few sample cutoff frequencies. Note that removing every additional frequency line corresponds to increasing the cutoff frequency f_{cut} by $1/600 = 0.00167$ Hz.

The R^2's for single-parameter regressions on V, σ_{high} and I_{high} as well as those for the joint regression have been plotted vs. f_{cut} in Figure 4. V, which does not change with filtering, has a constant R^2 across different cutoff values. The standard deviation, however, which performs rather poorly before any filtering is done, quickly becomes an important parameter after a few frequency lines are filtered—to the degree that, for cutoffs greater than .005 Hz, $R^2_{\sigma_{high}}$ becomes larger than the R^2 for the joint regression (when the latter is adjusted for using an extra parameter, as discussed in motivating Eq. 10). The plot also confirms our expectation that σ_{high}, when considered individually, would be a more important parameter that I_{high}.

For a frequency cutoff of .15 Hz, the regression

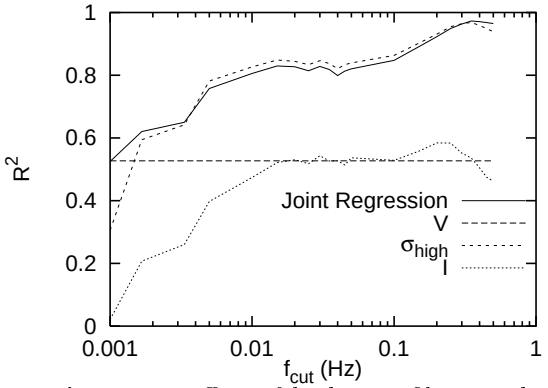

Figure 4: Effect of high-pass filtering the wind speed on R^2 for $f_0\overline{S}$ (NPS data).

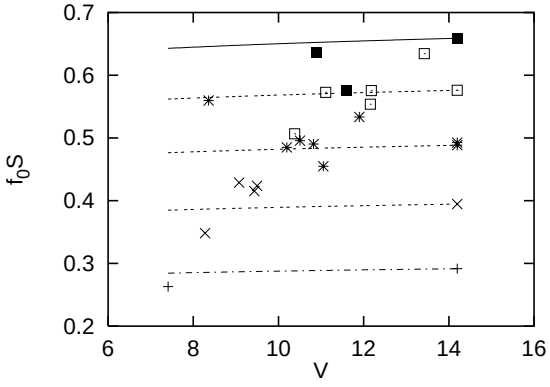

Figure 5: Joint regression of $f_0\overline{S}$ on V and σ_W plotted vs. V. Frequencies less than .15 Hz have been removed from the wind.

surface and the data points have been plotted vs. V and σ_{high} and are shown in Figures 5 and 6. These plots have the same format as Figures 2 and 3. However, comparing the two sets of plots reveals an important difference between them: while the slope vs. V is much larger than that vs. σ_W in the first set, after filtering the trend with σ_{high} has become more important than that with V. This result could have been guessed from the R^2 values as well, the R^2 for the joint regression being effectively equal to that for V alone when no filtering is done, and almost equal to that for σ_{high} alone by the time frequencies below .15 Hz are discarded. The change in the roles of V and σ is not difficult to explain if we are willing to believe, as indicated by Figure 4, that the filtered σ is the important factor in estimating the stress mean. Thus, if σ_{high} is used directly in the regression, one would not expect to see any remaining trend in V. However, this parameter is not used in the case of Figures 2 and 3. Thus the mean wind speed, being correlated with σ_{high}, is able to act as a proxy for it. Hence the apparent trend with V.

Higher Moments. $f_0\overline{S}$, which we have studied so far, is sufficient for fitting 1-parameter models to the stress data. However, to test the adequacy of such models in representing the data, and to fit 2- or 3-parameter models if simpler ones prove insufficient, information about the "shape" of the distibution—as reflected in the higher moments—is required. We will use *normalized* moments for this purpose:

$$\mu_2 = \frac{\sqrt{E[(S-\overline{S})^2]}}{\overline{S}} \tag{15}$$

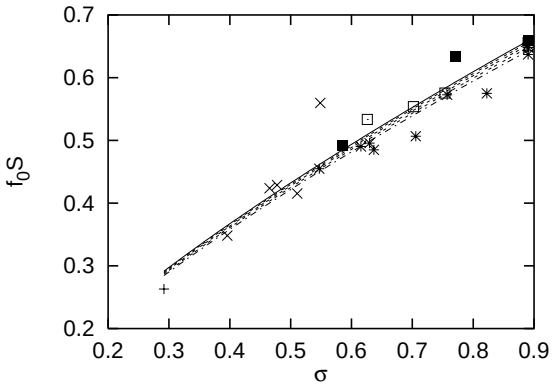

Figure 6: Joint regression of $f_0\overline{S}$ on V and σ_W plotted vs. σ_{high}. Frequencies less than .15 Hz have been removed from the wind.

i.e., the Coefficient of Variation; and,

$$\mu_3 = \frac{E[(S-\overline{S})^3]}{\sigma_S^3} \tag{16}$$

i.e., the skewness.

Analysis similar to that performed for $f_0\overline{S}$ can be employed to study the correlation between these moments and the various wind parameters discussed. A plot of the resulting R^2 values is shown for each of these moments in Figures 7 and 8. These values, as can be seen from the plots, are strikingly low—even negative in the case of μ_2. The skewness, in general, has higher R^2's, but even the maximum values—lying in the .30-.40 range—cannot be considered very significant. These results indicate that, based on the data at hand, little benefit can be expected from the regression.

The low R^2 values do not neccessarily indicate a large scatter in the data. The CoV's of the higher

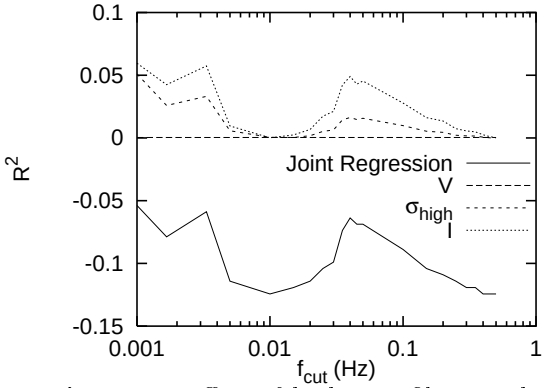

Figure 7: Effect of high-pass filtering the wind speed on R^2 for the CoV (NPS data).

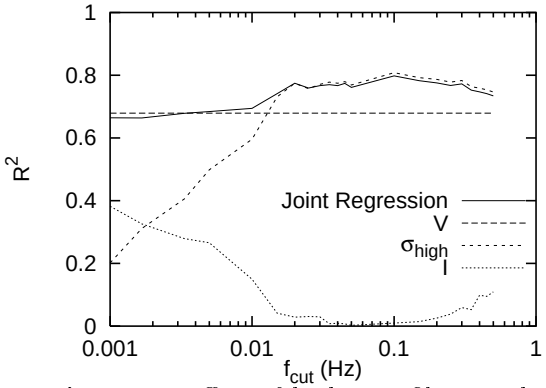

Figure 9: Effect of high-pass filtering the wind speed on R^2 for the WTS-4 turbine.

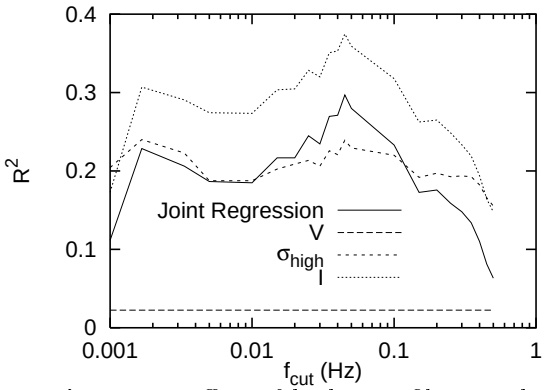

Figure 8: Effect of high-pass filtering the wind speed on R^2 for the skewness (NPS data).

moments, roughly .05 for μ_2 and .10 for μ_3, show that there is not much scatter in the data that needs to be explained through regression. This suggests that the shape of the distribution is not highly dependent on the wind condition, and a distribution with fixed CoV and skewness (equal to the mean of the values obtained from the data) can be used to model the stresses. The mean values $\overline{\mu_2} = 1.1$ and $\overline{\mu_3} = 1.8$ for this data set are close to $\mu_2 = 1$ and $\mu_3 = 2$ for the exponential distribution.

Other Turbines. The results presented so far have all been obtained for the NPS machine. To study the generality of the observed trends, we now present the results obtained for two additional wind turbines. We focus on $f_0\overline{S}$ since the previous results indicate that this moment has the greatest variability and is best correlated with the wind.

The additional turbines are both 2 bladed, downwind, teetered, constant speed horizontal-axis wind turbines. The first—the WTS-4—has a power rating of 4 megawatts, active yaw, and full-span variable-pitch control. Each blade is 38 meters long, and the normal operation speed is 31 rpm. The next—the AWT-27—has a power rating of 275 kilowatts, free yaw and fixed pitch, and is stall controlled. The rotor diameter is 27 meters and the normal operating speed is 53.3 rpm. 42 10-minute segments of stress and wind speed data sampled at 10 Hz were available for each of the machines. However, in the case of the AWT-27, the method employed for measuring the wind speed had effectively reduced the resolution to 1 Hz.

The R^2 of $f_0\overline{S}$ is plotted vs. the cutoff frequency f_{cut} for the two machines in Figures 9 and 10. Notice the considerable difference between the two figures. While the trend observed for the WTS-4 data set is in general quite similar to that for the NPS data, the AWT-27 exhibits a completely different behavior. For this turbine $f_0\overline{S}$ is so highly correlated with the mean wind speed that little remains to be done by other parameters. This is clearly indicated by $R^2_V = .99$. Notice that even in this case there is a considerable correlation with σ up to $f_{cut} \approx .30$ Hz, after which the sudden decrease in R^2 indicates that important frequency components have been filtered out. The smaller correlation with σ_{high} could be in part due to the limit on the maximum observable frequency, created by the low sampling rate. This, however, does not explain the high correlation with the mean wind speed, which is independent of the sampling rate.

The WTS-4 machine, on the other hand, exhibits characteristics quite similar to those observed for the NPS (Figure 4). However, for the WTS-4 turbine the increase in R^2_σ due filtering is not as significant,

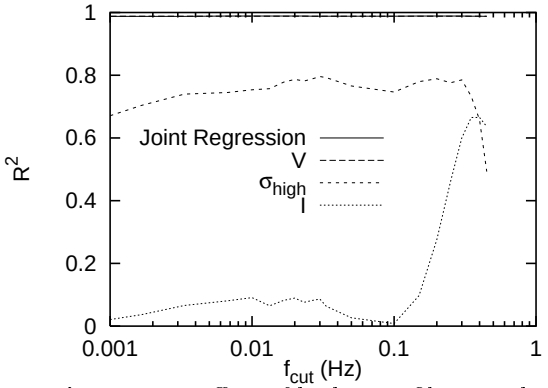

Figure 10: Effect of high-pass filtering the wind speed on R^2 for the AWT-27 turbine.

the maximum value being about .80 (compared to more than .95 for the NPS machine). One possible explanantion for this difference could be that the WTS-4, having a much larger rotor diameter (78 meters vs. 18 meters for the NPS machine) is more sensitive to the spatial variations in the wind speed, which are not captured in the present analysis.

The differences in the results obtained for these data sets can be due to the many differences that exist between the machines (e.g., differences in scale or other mechanical properties), their location (the AWT-27 and NPS turbines were installed within operating wind parks and complex terrain whereas the WTS-4 was operating alone without any turbines upstream in smooth terrain), and the way that the data were collected (such as the frequency of sampling). These observations indicate that the "important" environmental parameter is machine-dependent, and certain parameters may be useful in some cases but less so in others. Hence a study of the R^2 values is neccessary to determine the relevant parameter on a case by case basis.

Summary

Rainflow counted load amplitudes are summarized through their first three statistical moments and multiple regression analysis is applied to estimate the moments in various wind conditions. These moments can then be used to fit a 3-parameter quadratic Weibull distribution (or simpler 1- and 2-parameter models) to the stress ranges from which damage estimates can be made.

In this paper, the correlation of various wind parameters with the moments was studied and the following results were obtained:

- A measure R^2—the percentage of variance explained by the regression—was introduced for comparing different wind parameters in terms of their power to estimate the moments. Three wind parameters—V, I and σ_W—were compared using this measure, but none were found to be highly correlated with the moments.

- A new turbulence measure σ_{high} was obtained by removing a portion of the low-frequency content of the wind speed. In the case of two of the 3 HAWTs studied, this parameter was shown to be better correlated with the first moment. Removing even a few (3-5) frequency lines was found to be helpful in achieving better correlation. Although this turbulence measure does not reflect spatial variations, and thus cannot be considered as providing complete turbulence information, it was shown to provide a better parameter in the common situation of a single anemometer. Joint regression on V and σ_{high} indicated that the apparent trend with V—when no filtering is performed—is due to its correlation with the filtered turbulence σ_{high}.

- For a third HAWT, the mean wind speed proved to be the most important wind parameter. This difference in behavior suggests that the effectiveness of different wind parameters may be case dependent.

- The higher moments, i.e., the CoV and skewness, were found not to have much correlation with any of the wind parameters studied. However, these moments seem to have smaller variations than the first moment, suggesting that the shape of the stress distribution is not highly dependent on the wind conditions.

Similar studied are being done for edgewise moments. Further studies are needed to propagate the uncertainties in the moments to find the implied effect on design safety factors.

References

Barnard, J.C. and Wendell L.L. " A Simple Method of Estimating Wind Turbine Blade Fatigue at Potential Wind Turbine Sites," *Journal of Solar Energy Engineering*, Vol. 119, No. 1, ASME, February 1997

Connell, J.R., Morris, V.R., Powell, D.C., and Glower, G.L., "The PNL Single-Tower Measurement

Model of Rotationally Sampled Turbulent Wind, with User's Guide for STRS2PC," *PNL–6580,* Pacific Northwest Laboratories, Richland, WA, 1988.

Jackson, K.L, "Deriving Fatigue Design Loads from Field Test Data, *WindPower '92,* AWEA, 1992.

Jha, A.K., and Winterstein, S.R., "CYCLES 2.0: Fatigue Reliability Models and Results for Wave and Wind Applications," *RMS Report 27,* Reliability of Marine Structures Program, Civil Eng. Dept., Stanford University, 1997.

Kashef, T., and Winterstein, S.R., "Estimating Wind Turbine Blade Loads from Environmental Parameters," to be published: *SNL Report,* Sandia National Laboratories, Albuquerque, NM, 1997

Kelley, N.D., "A Comparison of Measured Wind Park Load Histories with the WISPER and WISPERX Load Spectra, *Wind Energy 1995,* ASME, SED Vol. 16, 1995.

Kelley, N.D., "The Indentification of Inflow Fluid Dynamics Parameters That Can Be Used to Scale Fatigue Loading Spectra of Wind Turbine Structural Components," NREL/TP-442-6008, National Renewable Energy Laboratory, Golden, CO, Nov. 1993.

Lange, C.H. and Winterstein, S.R. "Fatigue Design of Wind Turbine Blades: Load and Resistance Factors from Limited Data," *Energy Week—Wind Energy Symposium,* ASME, SED Vol. 17, 1996.

Veers, P.S., "Blade Fatigue Life Assessment with Application to VAWTs," *Journal of Solar Engineering,* ASME, Vol. 104, No. 2, May 1982.

Veers, P.S. and Winterstein, S.R., "Application of Measured Loads to Wind Turbine Fatigue and Reliability Analysis," *1997 ASME Wind Energy Symposium,* AIAA, 1997.

Winterstein, S.R. and Lange, C.H., "Load Models for Fatigue Reliability from Limited Data," *Wind Energy 1995,* ASME, SED Vol. 16, 1995.